Chapter 3

Damage Detection Techniques

3.1. Introduction

In this chapter, various conventional and unconventional techniques for SHM have been presented and discussed. The chapter starts with the introduction of the strain gauge method to obtain the strain values in the structure. Finite Element Method is also being widely used for SHM and strain measurement. This method is also discussed in brief. The use of a fiber optic sensor for strain measurement is also drawing the attention of the researchers, and the same is discussed in detail. Neural network technology integrated with the fiber optic sensor for the damage detection within the structure has also been presented. Fundamentals of wavelet and their application in damage analysis based on the diffused wave have also been discussed.

3.2. Strain Gauge Method

Strain gauges are the most commonly used strain measurement technique. Advantage of using strain gauges include good accuracy, low cost, and flexibility in use. Strain gauges are resistive sensors used for strain measurement of the structure at the point of contact. The strain gauge works on the principle that the change in physical parameters of a wire used in the strain gauge changes the resistance of the wire. By measuring this change in resistance, change in the physical variable can be predicted. The physical variable in the present work corresponds to strain(ε).

$$\varepsilon = \frac{\Delta L}{L} \tag{3.1}$$

The resistance of the wire is given by

$$R = \rho \frac{L}{(A_c)} \tag{3.2}$$

Where ρ the resistivity of the material, L is is the length of the wire, and (A_c) is the area of the cross-section of the wire. As the resistivity of the wire is constant, so the resistance of the wire is a function of length and cross-section area of the wire. Any change in the above parameters corresponds to the change in the resistance. On applying the load on the structure, the change in the above parameters occurs, which causes the change in the resistance of the strain gauge.

Strain gauges are utilized in a Wheatstone bridge, which comprises four resistors in an electrical circuit. One of the resistors is supplanted with a strain gauge(quarter connect), and the subsequent circuit can be utilized to quantify the strain of the structure. Be that as it may, because of certain estimating vulnerabilities under the impact of electric and magnetic fields, it gives arbitrary fault measurements that influence its exactness. Similarly, legitimate working of the strain gauge relies upon the contact of strain gauge with the smple, and so the same should be done carefully.

3.3. Finite Element Methodology

With the urge of advancement, finite element analysis came into existence in the late 1950s. It is a method to solve structural problems with complex geometry. The basic fundamental of this method is the discretization of large structures into sub-structures known as elements. Different finite element methods include Rayleigh, Ritz, and

Galerkin. Through different stages of development, finite element analysis has emerges as a popular tool in area of engineering and research. This technique is now considered as an integral part of structural analysis. The finite element has also been used in the present research, which will be discussed in detail in the later chapters.

3.4. Fiber Optic Sensor technology

Despite the fact that the advancement of fiber optic-based structural health monitoring is noteworthy, it is yet to arrive at its maximum capacity, particularly as far as market abuse. One of the energizing fields wherein FOS's and health monitoring are relied upon to assume a noteworthy job is smart structures and intelligent systems. Fig. 3.1 summarizes different sensor technologies used in structural health monitoring.

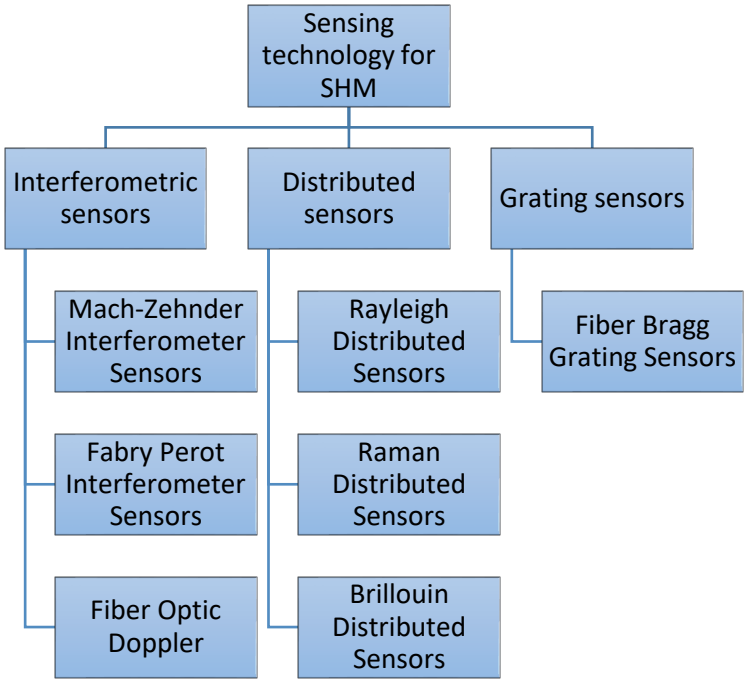

Fig. 3.1. Block diagram of different fiber optics sensor technologies

An interferometric optical-fiber strain sensor gauges the relative hindrance between the light going in its reference and detecting arms and afterward relates the retardation or phase shift to the strain. The applied strain field influences the refractive index, which thus changes the phase shift. The phase shift is likewise delivered along the check length of the fiber. There likewise exists an optical path length change brought about by the waveguide-mode scattering, yet it is insignificant in the surface-mounted optical fiber sensors. For the straight fibers, Butter and Hocker introduced a relation, as given in Eq. 3.3, between the changes in the phase to the axial fiber strain [81].

$$\Delta\emptyset = \frac{2\pi n_0 L}{\lambda}\left[1 - \frac{n_0^2}{2}\{P_{12} - \nu_f(p_{11} + p_{12})\}\right]\varepsilon_n \qquad (3.3)$$

The above equation is valid only when a straight fiber segment is exposed to a constant or a linear strain field case. However, the "ε_n" is the average axial strain over the active fiber length. Further, Butter and Hocker assume that only axial strain components in the fiber significantly affect phase change and dominate the phase shift in optical-fiber hydrophones. The excitation is applied to the detecting fiber, bringing about an optical path contrast between the reference and detecting fiber strands. The light intensity of the yield of the Mach-Zehnder interferometer can be communicated as,

$$I = 2A^2[1 + \cos(\Delta\emptyset)] \qquad (3.4)$$

$$\Delta\emptyset = \frac{2\pi n_0}{\lambda}\left[1 - \frac{n_0^2}{2}\{P_{12} - \nu_f(P_{11} + P_{12})\}\right]\int_{L_f} \varepsilon_f dx \qquad (3.5)$$

Expanding equation 3.3 for strain in active length of optical fiber we get equation 3.5. Since the terms outside the integration sign of equation 3.5 are constants for any given optical fiber system, the total optical phase shift is proportional to the optical fiber strain. By measuring the total optical phase shift, the optical fiber strain can be easily obtained as follows:

$$\int_{L_f} \varepsilon_f dx = \frac{\Delta \emptyset}{\frac{2\pi n_0}{\lambda}\left[1 - \frac{n_0^2}{2}\{P_{12} - \nu_f(P_{11} + P_{12})\}\right]} \tag{3.6}$$

The strain obtained from equation 3.6 denotes the strain in the sensing length of the fiber, which is surface bonded onto the host structure. The average strain of the optical fiber for optical phase shift is:

$$\varepsilon_{avg} = \frac{\int_{L_f} \varepsilon_f dx}{L_f} = \frac{\Delta \emptyset}{\frac{2\pi n_0}{\lambda}\left[1 - \frac{n_0^2}{2}\{P_{12} - \nu_f(P_{11} + P_{12})\}\right]} \tag{3.7}$$

The relative retardation can be delivered in a Mach-Zehnder design. The Mach-Zehnder position disentangles the sensor structure, yet it additionally seriously restricts the adaptability of the sensor. A strain-free reference fiber would be hard to keep up outside a research laboratory. In the applications considered here, the detecting fiber arms are presented to the strain field by bonding them to the outside of a stressed structure.

Fabry-Perot interferometric sensors are particularly suited to measure very low strains in large scale infrastructures. Examples of such applications are the measurement of

small strains or vibrations in large structures like rocket test stands, buildings, oil rigs, bridges, dams, etc. Fabry – Perot is referred to as a spectrum analyzer where the transmission occurs according to eq. 3.8 [90]. As intensity is proportional to the square of the modulus of the electric field amplitude, so transmitted intensity I_T in terms of incident wave intensity I_0 can be related as given in equation 3.8.

$$I_T = \frac{I_0(1-r)^2}{(1+r^2-2r\cos 2\delta)} = \frac{I_0(1-r)^2}{(1-r)^2-4rsin^2\delta} \tag{3.8}$$

Where r is the ratio of the intensity of refracted and incident ray, and δ is the phase parameter of the incident light. The strain is then calculated by using equations 3.4 through 3.8.

A Doppler impact based fiber-optic (FOD) sensor depends on the Doppler impact of lightwave transmission in optical fiber, and it works as a vibration/acoustic sensor. The Doppler shift in the frequency can be gotten from the accompanying condition [91].

$$f_D = -\frac{n}{\lambda_0} \cdot \frac{dL}{dt} \tag{3.9}$$

Where λ_0 is the light wavelength in the vacuum, and λ_0/n is the light wavelength in the optical fiber. Doppler frequency shift f_D of a circular loop FOD can be used to obtain the axial strain in fiber using following equation [90].

$$f_D = -\frac{\pi nq}{\lambda_0} \cdot (\dot{\varepsilon_x} + \dot{\varepsilon_y}) \tag{3.10}$$

Another detecting innovation utilized for FOS incorporates distributed sensors. On account of these sensors, the incident electromagnetic field will reorient the initially indistinguishable irregular fluctuating atomic mists. This inclination of re-direction has watched all things considered on a small spatial scale covering a small part of the frequency. Such an aggregate inclination to react to an EM field would bring about macroscopic polarization that corresponds to the external electric field. A portion of the dissipated Rayleigh light is re-captured by the waveguide and sent in a regressive path. On account of Rayleigh distributed sensors, the regressive spreading Rayleigh dispersed light has a period of delay that can be utilized for distributed detecting. The uses of Rayleigh dispersing to the fiber detecting are generally wide-coming; it tends to be utilized to detect local temperature or strain through identifying obstruction comparative with a reference length. It can likewise be utilized to detect impact vibrations.

The Raman dispersing depends on inelastic interaction systems between the propagating light pulse and the optical fiber. Photons of a pulse laser are infused into an optical fiber and the exchange of energy with the molecules of the fiber material occurs. New photons with lower or higher energy are then delivered, and the backscattered spectrum is made out of two pinnacles or groups called Stokes and Anti-Stokes parts. Utilizing the proportion of the intensities of Stokes and Anti-Stokes segments, the thermal strain can be found.

Another distributed detecting innovation incorporates Brillouin scattering. In this sensor, excitation can be produced specifically at a particular segment along the fiber. The selected segment can be differed by adjusting the frequency modulation to accomplish dispersed estimation. In Brillouin Optical Correlation Domain Analysis

(BOCDA), the position to be estimated can be chosen arbitrarily along the fiber. Brillouin dynamic grating (BDG), an acoustic-wave created refractive-index grating caused in the simulated Brillouin dissipating process, produce Bragg reflection for the symmetrically polarized light wave in a polarization-maintaining fiber. Estimation of BDG, just as the Brillouin dispersing, synchronous appropriated estimation of strain, and temperature, have been acknowledged by the BOCDA. Fiber optic nerve frameworks, to be specific circulated and multiplexed optical fiber detecting innovations, are valuable to cause the structures and materials to anticipate the damage and defects. Brillouin and Rayleigh's scatterings are subtle to both temperature and strain, while Raman dispersing is just delicate to temperature.

Another well-known optical detecting innovation incorporates grating sensors. Under phase coordinating conditions, a fiber Bragg grinding (FBG) couples the forward engendering core mode to the regressive proliferating core mode. A long fiber grating (LPG) can couple the forward proliferating core mode to one or a couple of the forward engendering cladding modes. A chirped fiber grating has a more extensive reflection range, and every frequency component is reflected at various positions, which brings about a defer time distinction for various reflected frequencies. A tilted fiber grinding can couple the forward spreading core mode to the retrogressive proliferating core mode and a regressive engendering cladding mode. An inspected fiber grating can mirror a few frequency components with equivalent frequency dividing. Every one of these kinds of gratings have been used in different sorts of fiber grinding sensors and frequency change cross interrogators.

3.5. Analytical explanation of Fiber Optic Strain Sensors

The basic working of the optical strain sensor is based on a strain-induced phase shift that occurs in the light signal being transmitted in an optical fiber. Sirkis and Haslach showed that only the axial component of strain in a surface-mounted optical fiber affects the index of refraction [82]. Elemental analysis is performed to obtain the relation between the change in phase with the variation in the index of refraction along the length of the fiber. For a small elemental segmental length (Δs), the index of refraction is approximated as a constant equal to n(s). Phase change relation exists, as shown in equation 3.11.

$$\Delta\emptyset = \frac{2\pi}{\lambda} n(s)(1+\varepsilon_n)\Delta s \tag{3.11}$$

Limiting the value as Δ→0 we get

$$\frac{d\emptyset}{ds} = \frac{2\pi}{\lambda} n(s)(1+\varepsilon_n) \tag{3.12}$$

On integrating equation 3.12 along the length of the fiber

$$\emptyset = \frac{2\pi}{\lambda} \int_0^L n(s)(1+\varepsilon_n)\, ds \tag{3.13}$$

Equation 3.13 shows that phase is an increasing function with L. Index of refraction in a surface-mounted fiber is a function of ε_n. Equation 3.14 shows the first-order terms

$$n(s) = n_0 (1 - c\varepsilon_n) \tag{3.14}$$

Where n_0 index of refraction under the unstrained condition and c is defined as

$$c = \frac{n_0^2}{2}\{p_{12} - \nu_f(p_{11} + p_{12})\} \tag{3.15}$$

Where p_{ij} is pockel's constant and ν_f is the Poisson's ratio. Now assuming $\beta = 2\pi n_0/\lambda$ and ignoring higher-order terms we get

$$\emptyset = \beta \int_0^L (1 - c\epsilon_n)(1 + \epsilon_n)\, ds = \beta L + \beta(1 - c) \int_0^L \epsilon_n ds \tag{3.16}$$

Butter and Hocker strain equation (eq. 3.17), is obtained by subtracting the phase values obtained from equation 3.19 for the strained and unstrained condition [81].

$$\Delta\emptyset = \beta(1 - c) \int_0^L \varepsilon_n ds = \beta(1 - c)\, \varepsilon_{avg.} \tag{3.17}$$

Where $\varepsilon_{avg.}$ is average strain developed in optical fiber. To develop a sensor design using this phase change property of optical fiber, the sensing and reference path have been expressed as a function of optical parameter t_s. Sensing and reference path can be expressed in x-y co-ordinate system as shown in equation 3.18.

$$f_s(t_s)=[x(t_s), y(t_s)], \qquad f_r(t_r)=[x(t_r), y(t_r)] \tag{3.18}$$

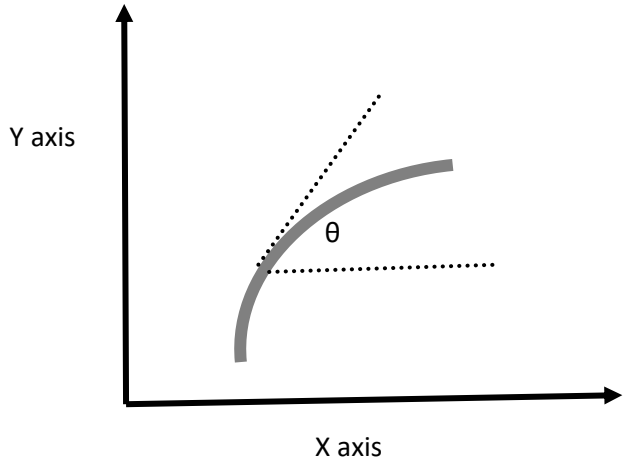

Fig. 3.2. Co-ordinate axis position for fiber curve

Assuming a fiber position in x-y co-ordinate at angle θ tangent to the fiber curve as shown in the fig. 3.2.taking tangent of the axis as

$$tan\theta = y'/x' \tag{3.19}$$

Where $y' = dy/dt$ and $x' = dx/dt$ therefore

$$Sin\ \theta = y'/\sqrt{x'^2 + y'^2} \quad , \quad Cos\ \theta = x'/\sqrt{x'^2 + y'^2} \tag{3.20}$$

Using strain transformation law

$$\varepsilon_n = \epsilon_{xx} Cos^2\theta + \epsilon_{yy} Sin^2\theta + \gamma_{xy} \sin\theta \cos\theta \tag{3.21}$$

By using equation 3.20, and rearranging we get

$$\varepsilon_n = \frac{(\varepsilon_{xx} x'^2 + \varepsilon_{yy} y'^2 + \gamma_{xy} x' y')}{(x'^2 + y'^2)} \tag{3.22}$$

Length of the arc *s* of fiber path is related to the co-ordinate parameters as

$$ds = \sqrt{x'^2 + y'^2}\, dt \tag{3.23}$$

Substituting equation 3.16 and equation 3.17 in equation 3.11 we get

$$\Delta\emptyset = \beta(1-c) \int_0^L \varepsilon_n ds$$

$$= \beta(1-c) \int_0^L \frac{(\varepsilon_{xx} x'^2 + \varepsilon_{yy} y'^2 + \gamma_{xy} x' y')}{(x'^2 + y'^2)} \cdot \sqrt{x'^2 + y'^2}\, dt \tag{3.24}$$

For simplifying above integral we assume

$$k_1 = \int_0^L \frac{x'^2}{\sqrt{x'^2 + y'^2}}\, dt \quad , \quad k_2 = \int_0^L \frac{y'^2}{\sqrt{x'^2 + y'^2}}\, dt \quad ,$$
$$k_3 = \int_0^L \frac{x'y'}{\sqrt{x'^2 + y'^2}}\, dt \tag{3.25}$$

Now equation 3.24 simplifies as

$$\Delta\emptyset = \beta(1-c)\,[\epsilon_{xx}k_1 + \epsilon_{yy}k_2 + \gamma_{xy}k_3] \tag{3.26}$$

Applying co-ordinate conditions at $y'=0$, $k_2 = k_3 = 0$, thus above equation 3.26 became

$$\Delta\emptyset = \beta(1-c)\,[\epsilon_{xx}k_1] \tag{3.27}$$

From equation 3.27 it is clear that change in phase is directly related to the change in the axial strain for a surface-mounted fiber optic sensor.

The important characteristic to address in a transmission system is the noise performance of the system. There are different sources of noise in a communication system. The initial source of noise arises from the circuit itself, which is known as internal noise. The significant effect of noise has been observed at higher frequencies, and laser diodes operate at comparatively high frequencies; therefore, it becomes important to recognize noise in high-frequency transmission. Fluctuations in light intensity of laser output can be carried as noise in transmission signals. Reflection noise is a laser noise which occurs due to the Fresnel reflection phenomenon. The output

signal from a laser carries a specific wavelength, satisfying both gain and phase condition between two reflecting laser regions. But due to finite spectral width in the output of a laser, noise is generated, which is known as mode partition noise.

Speckle patterns are characteristically defined as a redistribution of power over the cross-section of the optical fiber core. But due to different wavelength components in the optical signal, it undergoes different phase changes with respect to time. The speckle pattern also varies with respect to time. This variation with time and the non-uniform power detection capability of the photo-detector over its entire cross-section create fluctuations in the output signal. This noise is called speckle noise. Relaxation oscillations produced at the receiver output also contribute to the increment in the noise of transmitting signals.

From the above discussion, it can be concluded that the practical use of the analytical solution for strain calculation may lead to some errors due to noise in the signals. There exist various methods to remove noise data using filters and other software. These signals can be successfully used to determine strain values using neural network technology. Neural network technology is cheaper and practically applicable to different problems that require data mining [83].

Calculation of strain using surface-mounted optical sensor given in equation 3.30 provides analysis only in static loading conditions. Under dynamic loading, the results of the analytical analysis may provide diverging results. Moreover, the noise in the signals also contributes to the variation of results, but the same signals can be successfully used to determine strain values using neural network technology.

3.6. Fundamentals of Neural Network Integrated FOS Based SHM for Damage Detection

Damage assessment is one of the important applications of fiber optic sensors in the area of structural health monitoring. The operation and mechanical compatibility of a sensor is the pre-requirement in a smart monitoring system. The advance structural health monitoring system requires a multidisciplinary understanding of various areas, which include mechanical, system engineering, sensing, actuation, and signal processing. Ye Lu et al. proposed an inverse analysis for damage identification in metal plates. Parametric modeling is used for finite element analysis to create a damage scenario with selected parameters. Mapping technique is applied to constitute damage parameter data, which includes digital damage fingerprints [49]. D.N Thatoi et al. expanded his work by proposing an advance crack detection technique using cascade forward back propagation neural network methodology. A comparative analysis between analytical, FEA, and artificial intelligence-based damage assessment is performed. The proposed model successfully predicts the severity and location of damage [51]. M. Gordan et al. reviewed the data mining process applicable to structural health monitoring [53].

L. Xie et al. studied the crack growth process in ductile alloys based on dynamic neural network modeling. The design of the network model was based on the learning of crack opening stress and crack length growth. It was shown that a well-developed dynamic neural network model has a capability of crack growth estimation [55]. Ahmed A. Elshafey et al. introduced the neural network concept for the analysis of crack spacing. Two kinds of neural network namely, radial base and feed-forward back-propagation,

are used for crack analysis [56]. M. Mehrjoo et al. tested a practical application of a neural network model for damage analysis of a truss bridge structure. Natural frequencies and mode shapes were used as input parameters for detecting damage percentage as output [86]. M. Rajendra et al. proposed a new neural network based on complex spaces. Complex valued radial basis functions are used for multiple crack analysis in beam structure. These advance network methodologies are initially applied for damage identification, followed by accurate crack location [87].

Paulraj M.P. et al. discuss the damage detection in the metal plates using artificial neural networks. Impact testing is performed for generating the vibration patterns, and time-domain signals are proposed to extract the desired features. A comparison of healthy and faulty samples are performed based on the feature extraction algorithms [88]. S. Suresh et al. used model frequency parameters for the approximation of crack location and depth identification. Computed model frequencies are used in training the network for locating and sizing the crack model. In this study, a modular neural network comprising of a multilayer perceptron model and a radial basis model is applied for the health monitoring of structures [89]. D. Maity et al. introduced a damage assessment methodology using a neural network. Analysis of damage and healthy samples are used for training the network displacement. The strain values are taken as input values, and damage location parameters are approximated as output values [57].

3.7. Fundamental of wavelet and multiscale analysis

Wavelet mechanics emerges as a popular tool in fulfilling the requirement of continuous technological development and advancement demand. The use of wavelet transform with the development of partial differential equations made this technique

more effective for mathematicians and engineers. Wavelet mechanics can successfully be applied in the area of data compression, image processing, time series analysis, and signal conditioning.

This chapter includes the basics and fundamental understanding of theory related to wavelet mechanics. The focus of the study is made on discrete wavelet analysis as per the requirement and scope of the study. Advancement is made with a logical explanation for diffuse zone selection using wavelet analysis. Moreover, wavelet mechanics can be applied for coefficient extraction at different levels which can be further used as input for neural network analysis for structural health monitoring.

3.7.1. Wavelet – An Overview

The credit of initial work on the orthogonal function system goes to Alfred Haar (1910). His dissertation titled "On the theory of the orthogonal function systems" is based on the orthogonal system of functions, which further expands as the development of a set of rectangular basis functions. During the investigation of Brownian motion, Paul Levy discovered that scale varying (or Haar basis) function could be preferred over the Fourier basis function for detailing of subtle variations. Haar basis function gives a high degree of precision in modeling a function as it can be scaled into different intervals. Various researchers contributed to the advancement of function modeling. In 1982, Jean Morlet developed the technique of scaling and shifting of analysis window functions in analyzing acoustic echoes and termed it as wavelet. Morlet and Grossmann have developed wavelet transform by providing proper mathematical formulation for continuous wavelet. Various mathematicians like I.Daubechies, A. Grossmann, S. Mallat, Y. Meyer, R.A. DeVore, R. Coifman, V. Wickerhauser, and many more gave their remarkable contribution to the advancement of wavelet analysis.

The invention of a multiresolution analysis by Mayer (1987) and Mallat (1989) expanded the application of wavelet methodology. Multiresolution analysis based designing the scaling function of wavelet allows constructing mathematical grounded new functions. Variation of scaling and transformation of wavelet generates a family of the wavelet function. According to Daubechies (1988), the wavelet transform can be defined as, "A wavelet transform is a tool that cuts up data, functions or operators into different frequency components, and then studies each component with a resolution matched to its scale."

3.7.2. Wavelet Transform

The concept of wavelet transform includes two basic parameters, namely scaling and shifting. Scaling of a function $\psi(t)$ is referred as a process of stretching or shrinking of signal in time, which can be expressed as $\psi\left(\frac{t}{s}\right)\ s > 0$ where 's' is a scaling factor which is a positive value and it corresponds to the extent up to which given signal is scaled in time. The scaling factor is inversely proportional to the frequency with a constant of proportionality. This constant of proportionality is known as the center frequency of wavelet (C_f). Mathematically, the equivalent frequency can be defined as the following equation

$$F_{eq} = \frac{C_f}{s\ \delta t} \tag{3.28}$$

Where s is wavelet scale, and δt is the sampling interval. Stretched wavelet helps in identifying slow variations in a signal, whereas compressed wavelet helps in identifying abrupt change in the signal. Shifting is the phenomenon of delaying or

advancing the onset of the wavelet signal length. A shift in the wavelet can be represented as ϕ(t-k). It shows that the wavelet got shifted and centered at k. Broadly, there exist two types of wavelet transform describes as follows:

3.7.2.1. Continuous Wavelet Transform (CWT)

This wavelet is best suited for time-frequency analysis as these wavelets do not have negative frequency components. The output of continuous wavelet transform are coefficients, which are generally a function of scale-frequency or time. When a wavelet is scaled by a factor of 2 it reduces the equivalent frequency by an octave. The advantage of using continuous wavelet transform is that the results can be analyzed at intermediate scales within each octave, which helps in the fine-scale analysis. Each scaled wavelet is shifted in time along the entire length of the signal, and a comparison is performed with the original signal. The process is repeated for different scales resulting in the coefficients that are functions of the wavelet scale and shift parameter. The continuous wavelet transform furnishes the decomposition of the signal $x(t)$ onto a set of basis functions that are worked out by an inner product of $x(t)$ with a mother wavelet $\psi(t)$, expressed as

$$W\,x(u,s) = \frac{1}{\sqrt{s}}\int_{-\infty}^{\infty} x(t)\psi^{*}\left(\frac{t-u}{s}\right)dt = < x(t),\ \psi_{u,s}(t) > \qquad (3.29)$$

Where ψ^{*}denotes the complex conjugate of mother wavelet and symbol <,> denotes the inner product. The mother wavelet $\psi(t)$ can be real or complex. The time-domain signal is decomposed by time convolution with the scaled basis of function $\psi(t)$ called as simpler or daughter wavelets. Morlet wavelet provides the visualization of the

possible discontinuities in the signal. Continuous wavelet transform can be utilized in the area of time-frequency analysis and filtering of time localized frequency components.

3.7.2.2. Discrete Wavelet Transform

Discrete wavelet transform (DWT) is ideal for denoising and image compression as it helps in representing naturally occurring signals and images with less number of coefficients. The base scale for discrete wavelet transform is two. Different scales can be obtained by raising the base scale value to 2^j where j = 1, 2, 3..... Translation can be considered as the integer multiples of scaling parameter and can be represented as $2^j m$ where m = 1, 2, 3.....

Both these processes are termed as dyadic scaling and shifting. This type of sampling reduces redundancy in coefficients. The output of discrete wavelet transform gives the same number of coefficients as in the input signal; therefore, the computation cost is reduced.

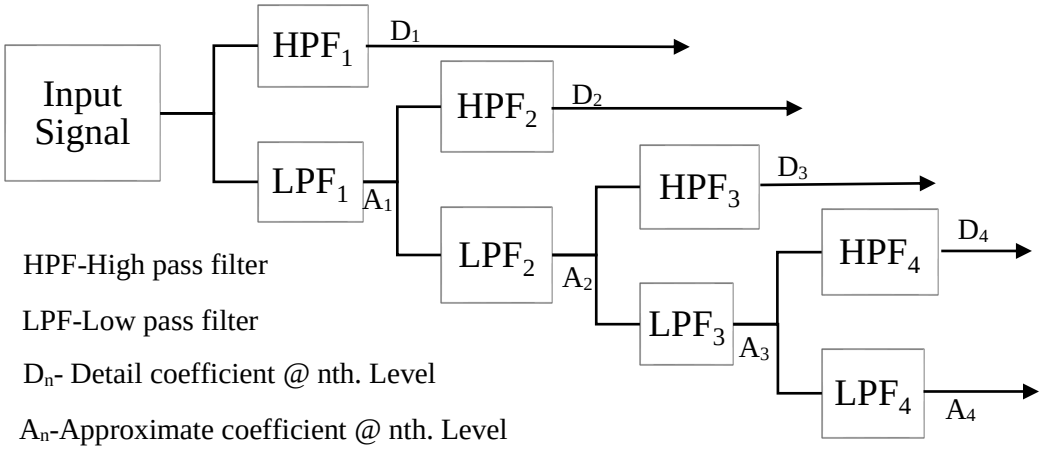

Fig. 3.3. Schematic showing working of discrete wavelet transform

As shown in fig. 3.3, the input signal is first filtered with a special low pass filter (LPF) and high pass filter (HPF) to give low pass sub-bands and high pass sub-bands, respectively. Half of the samples (data) are rejected after filtering as per Nyquist criteria. These filters carries high performance of computation as a consequence of small number of coefficients. These filters can also reconstruct the sub-bands while canceling the errors due to down sampling. The length of coefficients in each sub-bands is half of the number of coefficients in the preceding stage. In this way, a discrete wavelet helps in analyzing the signals at progressively narrow or sub-bands at a different resolution.

3.7.3. Signal Processing Using Wavelet Transform

Denoising a signal is the initial step in signal conditioning. In this section, the idea of denoising of the signal using wavelet is discussed. Further extension is given for the development of diffuse zone selection using wavelets. Basically, a discrete wavelet is applied in diffuse wave analysis. The decomposition of signal in detailed and approximated coefficients is carried out using multilevel wavelet decomposition. As DWT split signal into a low pass sub-band (approximation level) and high pass sub-band (detailed level), approximate sub-bands can be further decomposed at multiple levels or scales for fine-scale analysis. The next step is to analyze the detail coefficients and select the proper thresholding technique.

The first level detail coefficients capture the high frequency of the signal. Major components of the high frequency contain the noise of the signal, but a part of the high-frequency component can be made up of abrupt changes in the signal. Sometimes these abrupt changes carry meaning-full information, which can be useful in analysis.

Noise in the signal can be removed by the detail coefficients of using the threshold method. There exist two basic methodologies, namely soft and hard thresholding. In both cases, the coefficients with a magnitude less than the threshold value are set to zero. First soft-thresholding detail coefficients greater than the magnitude of threshold level are shrunken towards zero by subtracting the threshold value from coefficient value. In the case of hard-thresholding, the coefficients greater in the magnitude of threshold value are left unchanged.

3.8. Diffuse wave-based numerical analysis

Diffuse field analysis emerges as an alternate approach in the area of non-destructive evaluation of structures. Though diffuse signals are considered sensitive to the variations in the structural parameters, the difficulty exists in correlating ultrasonic response to the change in structural parameters. Conventional analytical methods used for quantitative comparison of diffuse signals include time-domain differencing and spectrogram differencing. A sincere advancement is made in the sequence of the above methods is a wavelet-based differencing method. The basis of all mentioned methods is the analysis of the energy difference between two signals. These energy parameters can be used for the successful detection of damage severity in a structure. Detail discussion related to energy methods is given in chapter 6.